PET imaging of carbonic anhydrase IX expression of HT-29 tumour xenograft mice with ^{68}Ga-labeled benzenesulfonamides.

Joseph Lau[1]†, Zhengxing Zhang[1]†, Silvia Jenni[1], Hsiou-Ting Kuo[1], Zhibo Liu[2], Daniela Vullo[3], Claudiu T. Supuran[3], Kuo-Shyan Lin[1,4]*, François Bénard[1,4]*

†These authors contributed equally to this work.

[1]Department of Molecular Oncology, BC Cancer Agency, Vancouver, BC, Canada
[2]Department of Chemistry, University of British Columbia, Vancouver, BC, Canada
[3]Università degli Studi di Firenze, Dipartimento Neurofarba and Laboratorio di Chimica Bioinorganica, Florence, Italy
[4]Department of Radiology, University of British Columbia, Vancouver, BC, Canada

***Corresponding Authors**
Dr. Kuo-Shyan Lin
Department of Molecular Oncology, BC Cancer Agency, 675 West 10th Ave,
Vancouver BC, Canada
klin@bccrc.ca
Phone: (604)-675-8208
Fax: (604)-675-8218

Dr. François Bénard
Department of Molecular Oncology, BC Cancer Agency, 675 West 10th Ave,
Vancouver BC, Canada
fbenard@bccrc.ca
Phone: (604)-675-8206
Fax: (604)-675-8218

Running title: CA-IX imaging with ^{68}Ga-labeled benzenesulfonamides

Keywords: Carbonic anhydrase IX, Hypoxia, Positron emission tomography, Benzenesulfonamide, Gallium-68

Conflict of interest: The authors declare no conflict of interest

Word count: 4914

ABSTRACT

Carbonic anhydrase IX (CA-IX) is a HIF-1-inducible enzyme that is overexpressed in many cancer subtypes to promote survival and invasion in hypoxic niches. Pharmacologic inhibition of CA-IX is achievable through sulfonamide-based inhibitors and has been shown to reduce primary growth of cancers and distant metastasis in preclinical models. We explored a multivalent approach for targeting CA-IX *in vivo*, non-invasively, with positron emission tomography. Three ^{68}Ga-labeled tracers containing either one, two, or three 4-(2-aminoethyl)benzenesulfonamide moieties were synthesized and evaluated for protein binding and imaging properties. Biodistribution and PET/CT imaging were performed using immunocompromised mice bearing CA-IX expressing HT-29 colorectal tumours. All three tracers allowed for the visualization of tumour xenografts at 1 h post-injection (p.i.), with the monomer displaying the highest contrast. Tumour uptake of the monomer was blockable in the presence of acetazolamide, confirming target specificity. The monomer was excreted predominantly through the kidneys, while the dimer and trimer were cleared by both renal and hepatobiliary pathways. According to biodistribution analysis, tumour uptake (%ID/g) of the monomeric, dimeric and trimeric tracers were 0.81 ± 0.15, 1.93 ± 0.26, and 2.30 ± 0.53 at 1 h p.i.. This corresponded to tumour-to-muscle ratios of 5.02 ± 0.22, 4.07 ± 0.87, and 4.18 ± 0.84 respectively. The successful development of CA-IX targeting PET tracers enables physicians to identify patients that will benefit from treatments targeting this protein.

INTRODUCTION

Tumour hypoxia has long been recognized as an impediment to radiotherapy and chemotherapy. Cancers that are hypoxic tend to be aggressive, with high propensity for distant metastasis (1). As hypoxia is a salient feature of most solid cancers, targeting components of the hypoxia-induced signaling cascade has been proposed as a means for oncologic treatment (2,3). The key enzyme mediating hypoxia-induced stress response in cancers is carbonic anhydrase IX (CA-IX). Regulated by hypoxia-inducible factors 1/2 (HIF1/2), CA-IX catalyzes the reversible hydration of carbon dioxide to bicarbonate ion (4,5). CA-IX promotes cancer cell survival by transporting bicarbonate ions into the cell to maintain pH homeostasis during glycolysis (4,5). Overexpression of CA-IX has been observed in a broad spectrum of cancers including: breast, cervix, ovarian, bladder, brain, colon, lung, kidney, head and neck, and oral cancers (2). In healthy individuals, CA-IX is expressed at low levels except in the gastrointestinal tract where it is involved in the process of cell differentiation (2). As CA-IX is pathologically expressed by cancer cells and located at the cell surface, it has emerged as a promising imaging/therapeutic target.

In preclinical settings, monoclonal antibodies and small molecule inhibitors have shown great promise in targeting CA-IX expressing cancers (2,6,7); however, there remains a need for an effective platform to screen for cancers that will respond to these drugs. As the most sensitive molecular imaging modality, positron emission tomography (PET) is well-suited for characterizing and quantifying expression of target proteins/oncogenes in primary lesions and metastatic sites. PET can detect the distribution of minimal amount (10^{-9}~10^{-12} mole) of radioisotope-tagged molecules in the body, non-invasively (8,9). In oncology, PET already plays an extensive role in diagnosis and staging, treatment planning, and treatment monitoring (10). With the introduction of novel radiotracers into the clinic, PET can provide valuable diagnostic information that can be readily integrated with pharmaceuticals to increase effectiveness and safety of cancer treatments (11). In the present study, we communicate the synthesis and biological evaluation of three ^{68}Ga-labeled sulfonamide derivatives for CA-IX molecular targeted PET imaging.

MATERIALS AND METHODS

Chemicals and instrumentation

All chemicals and solvents were obtained from commercial sources, and used without further purification. Proton NMR spectra were obtained using a Bruker (Billerica, MA) Avance 400inv spectrometer, and were reported in parts per million downfield from internal tetramethylsilane. Mass analyses were performed using a Bruker Esquire-LC/MS system with ESI ion source. Purification and quality control of ^{68}Ga-labeled CA-IX inhibitors were performed on an Agilent (Santa Clara, CA) HPLC system equipped with a model 1200 quaternary pump, a model 1200 UV absorbance detector, and a Bioscan (Washington, DC) NaI scintillation detector. The HPLC columns used were a semipreparative column (Phenomenex C18, 5 µ, 250 × 10 mm) and an analytical column (Eclipse XOB-C18, 5 µ, 150 × 4 mm). [^{68}Ga]$GaCl_3$ was eluted from either a 30-mCi ^{68}Ge/^{68}Ga generator from Eckert & Ziegler (Berlin, Germany) or a 50-mCi generator from iThemba LABS (Faure, South Africa). Radioactivity of ^{68}Ga-labeled tracers were measured using a Capintec (Ramsey, NJ) CRC®-25R/W dose calibrator, and the radioactivity of mouse tissues collected from biodistribution studies were counted using a Packard Cobra II 5000 Series auto-gamma counter. PET imaging experiments were conducted using a Siemens Inveon microPET/CT scanner (Malvern, PA).

Chemistry and radiolabeling

Synthesis scheme accompanied by detailed synthesis and radiolabeling procedures can be found in Supplemental Data section.

Binding affinity measurement

Inhibition constants (K_i) for CA-I, CA-II, CA-IX and CA-XII were determined with CA catalyzed CO_2 hydration assays following published procedures (12).

Stability in mouse plasma

Stability of the radiotracers were assessed in balb/c mouse plasma (Innovative Research) for 2 h at 37°C following published procedures (13).

Lipophilicity measurement

Measured octanol:water distribution coefficient at pH 7.4 ($LogD_{7.4}$) values

Cell lines and animal models

HT-29 human colorectal cancer cells were obtained as a gift from Dr. Donald Yapp (BC Cancer Research Centre, Vancouver, Canada). HT-29 cells were cultured in Dulbecco's Modified Eagle's Medium (Sigma) supplemented with 10% fetal bovine serum (Sigma), 100 U/mL penicillin-streptomycin (Thermo Scientific), and non-essential amino acids (Gibco). Cells were incubated at 37°C in an atmosphere containing 5% CO_2 and used for in vitro or in vivo experiments when 80-90% confluence was reached.

All animal studies were performed in accordance with the Canadian Council on Animal Care guidelines and approved by the animal care committee of the University of British Columbia. Male immunodeficient NOD.Cg-*Prkdc*^{scid}*Il2rg*^{tm1Wjl}/SzJ (NSG) mice bred in-house at the Animal Research Centre, BC Cancer Research Centre were used for this

study. Under anesthesia with 2.5% isoflurane in 2.0 L/min of oxygen, mice were subcutaneously inoculated with 5 x 10^6 HT-29 cells (in 100 µL PBS and BD Matrigel Matrix at 1:1 ratio) under the right dorsal flank. Biodistribution studies and PET/CT imaging were performed when tumours reached 7-9 mm in diameter.

PET imaging and biodistribution studies

PET imaging studies of ^{68}Ga-labeled tracers were conducted on HT-29 tumour bearing mice. Under 2.5% isoflurane anesthesia in oxygen at 2.0 L/min, 3.7-7.4 MBq of ^{68}Ga-DOTA-AEBSA, ^{68}Ga-DOTA-$(AEBSA)_2$ or ^{68}Ga-NOTGA-$(AEBSA)_3$ in a volume of 200 µL was administered intravenously through the caudal vein. For blocking experiments, mice were intravenously pre-injected with 10 mg/kg acetazolamide 1 h (100 – 200 µL in saline, i.v.) before administering the radiotracer. At 1 h p.i., a 10 min PET scan was performed using an Inveon micro PET/CT scanner. For anatomical localization, a 10 min CT scan was performed prior to each PET acquisition. Body temperature of mice was maintained at 37°C with the use of thermal pads. PET data were acquired in list mode acquisition, reconstructed using the 3d-OSEM-MAP algorithm with CT-based attenuation correction, and coregistered for dataset alignment. Three-dimensional regions of interests (ROIs) were placed on the reconstructed images to determine the %ID/g of tissue using the Inveon Acquisition Workplace software (conversion factor was predetermined using a germanium source).

Biodistribution studies were performed to confirm the quantitative ROI uptake values observed from PET scans. At 1 h p.i., mice were euthanized by CO_2 asphyxiation followed by cervical dislocation. Tissues of interest (blood, testes, stomach, intestine, spleen, liver, pancreas, kidney, lung, heart, tumour, muscle, bone and brain) were collected. Tissues were rinsed with PBS (except blood), blotted dry, weighed, and measured on a gamma counter.

Data Analysis

All statistics were performed using Prism 6 software (GraphPad). *P* values for the difference of tracer uptake in mouse tissues between unblocked and blocked groups were calculated using a Student's *t*-test (unpaired, one-tailed) and values < 0.05 were considered statistically significant.

RESULTS AND DISCUSSION

Rationale and design

Carbonic anhydrases are a large family of zinc metalloenzymes that share a highly conserved protein domain for catalysis (6). Inherently, the design of CA-IX selective imaging agents is hindered by potential off-target binding to other CA isoforms. Whereas most CAs are found intracellularly (ex. CA-I and CA-II are expressed in high abundance in erythrocytes), CA-IX and CA-XII are the two isoforms that reside at the extracellular surface (6,14). Although CA-XII is also ectopically expressed by cancers in response to hypoxia, it has lower expression profile and catalytic activity than CA-IX (14). Based on the spatial distribution of the various CA isoforms, small molecule inhibitors that are cell impermeable have enhanced selectivity for CA-IX. Different strategies to confer CA-IX selectivity include introducing bulk (fluorophores, albumin binders, glycosylation, multimeric design (15-19), net charge (pyridinio sulfonamides) (20,21), and/or enhancing hydrophilicity (polyaminocarboxylate chelators) (22-24). Rami *et al.* synthesized several series of aromatic sulfonamides conjugated to DTPA, DOTA, and TETA chelators for Cu^{2+} complexation, and proposed their application for ^{64}Cu PET imaging (22). Although these hydrophilic Cu^{2+}-polyaminocarboxylate-chelator complexes successfully prevented the sulfonamide inhibitors from entering erythrocytes, ^{64}Cu-DTPA/DOTA/TETA complexes are known to exhibit poor stability in vivo (25).

For our study, we synthesized monomeric (DOTA-AEBSA), dimeric (DOTA-$(AEBSA)_2$) and trimeric (NOTGA$(AEBSA)_3$) sulfonamide inhibitors and radiolabeled them with ^{68}Ga (Figure 1A). ^{68}Ga has a short radioactive half-life (67.7 min) that makes it suitable for labeling pharmaceuticals that have rapid targeting and clearance profiles (26). As an imaging isotope, ^{68}Ga decays 89% via positron emission with an average 740 keV ($E^{+}_{\beta max}$ = 1.899 MeV) positron energy per disintegration (26). ^{68}Ga-DOTA/NOTGA complexes are highly stable (27), and several ^{68}Ga-DOTA peptide derivatives have successfully entered the clinic setting for targeting somatostatin receptors in neuroendocrine tumours (28). More significantly, as ^{68}Ga can be eluted from $^{68}Ge/^{68}Ga$ generators for on-demand synthesis, this allows facilities without access to a cyclotron to readily synthesize these tracers. We hypothesized that this multivalent approach may increase binding avidity to CA-IX and afford cell impermeability through accumulation of molecular weight.

Conjugation of sulfonamide moieties to polyaminocarboxylate chelators does not hinder CA-IX binding and inhibition

Sulfonamide derivatives inhibit CA-IX enzymatic activity by forming coordination with Zn^{2+} ion of the catalytic domain and displacing H_2O (6). The primary concern with incorporating a multidentate chelator into our structural design was the possibility of steric hindrance. To ensure that our compounds can bind to CA-IX after coupling to either DOTA (monomer and dimer) or NOTGA (trimer), we first evaluated their binding affinity (K_i) using a CA catalyzed CO_2 stopped-flow hydration assay. K_i of Ga-DOTA-AEBSA, Ga-DOTA-$(AEBSA)_2$, and Ga-NOTGA-$(AEBSA)_3$ for CA-IX were determined to be 10.8, 25.4, and 7.7 nM, respectively (Table 1). For acetazolamide, a pan CA inhibitor, a K_i value of 25.0 nM for CA-IX was measured under the same assay conditions.

^{68}Ga-labeled tracers were obtained in high radiochemical yield, specific activity with good ex vivo stability

Results of the radiolabeling experiments are summarized in Table 1. All three tracers were successfully radiolabeled with ^{68}Ga with decay-corrected isolated yields of > 64% ($n \geq 3$). The specific activities measured were 536.5 ± 187.1, 269.5 ± 176.9, and 50.9 ± 8.4 GBq/µmol for ^{68}Ga-DOTA-AEBSA, ^{68}Ga-DOTA-$(AEBSA)_2$, and ^{68}Ga-NOTGA-$(AEBSA)_3$ respectively. After purification by radio-HPLC, tracers were obtained in ≥ 97.5% average radiochemical purity for in vitro and in vivo experiments. Stability of the tracers was assessed by incubating the tracers in mouse plasma. Tracers were highly stable in plasma, as > 90% of them remaining intact after for 2 h incubation at 37°C (Supplement Figure 2).

^{68}Ga-labeled sulfonamides generated modest-contrast images in CA-IX expressing tumour xenografts

Representative decay-corrected PET images of HT-29 tumour-bearing mice at 1 h p.i. are shown in Figure 4. Tracer uptake was observed in tumour xenografts for all three tracers. From the PET images, it is evident that the ^{68}Ga-DOTA-AEBSA is eliminated faster from non-target tissues than both the ^{68}Ga-DOTA-$(AEBSA)_2$ and ^{68}Ga-NOTGA-$(AEBSA)_3$. While ^{68}Ga-DOTA-AEBSA was excreted predominantly through the kidneys, ^{68}Ga-DOTA-$(AEBSA)_2$ and ^{68}Ga-NOTGA-$(AEBSA)_3$ were cleared by both renal and hepatobiliary pathways. The differences in pharmacokinetic profile may be attributed to tracer lipophilicity. The incorporation of each additional benzenesulfonamide moiety increased overall lipophicility. The measured octanol:water distribution coefficient at pH 7.4 ($LogD_{7.4}$) were -4.37 ± 0.08, -3.52 ± 0.01, and -2.39 ± 0.01 for ^{68}Ga-DOTA-AEBSA, ^{68}Ga-DOTA-$(AEBSA)_2$, and ^{68}Ga-NOTGA-$(AEBSA)_3$, respectively (Table 2). As ^{68}Ga-DOTA-AEBSA generated the highest contrasted images, blocking studies were performed by pre-injecting acetazolamide (10 and 20 mg/kg, intravenous) before tracer administration. Uptake in HT-29 tumours was successfully blocked compared to baseline studies indicating tracer specificity (Figure 3).

Biodistribution analysis corroborated observations of the PET images (Table 3). Tumour uptake of ^{68}Ga-DOTA-AEBSA, ^{68}Ga-DOTA-$(AEBSA)_2$, and ^{68}Ga-NOTGA-$(AEBSA)_3$ were 0.81 ± 0.15, 1.93 ± 0.26, and 2.30 ± 0.53 %ID/g at 1 h p.i.. Absolute uptake appeared to correlate positively with the number of targeting moieties as well as molecular weight of the tracers. For ^{68}Ga-DOTA-AEBSA, minimal uptake was noted in non-target tissue with kidneys being the only organ with higher uptake (4.37 ± 1.04 %ID/g) than tumour at 1 h p.i. For ^{68}Ga-DOTA-$(AEBSA)_2$ and ^{68}Ga-NOTGA-$(AEBSA)_3$, enhanced tumour uptake is accompanied by an increase of radioactivity in kidneys (14.84 ± 7.21 and 14.40 ± 1.65) and in liver (3.78 ± 1.06 and 8.01 ± 3.58). Uptake in latter indicated the involvement of the hepatobiliary pathway in the excretion profiles of both the dimer and trimer. Pre-injection with 10 mg/kg of acetazolamide significantly reduced the uptake of ^{68}Ga-DOTA-AEBSA in tumours to 0.41 ± 0.10 %ID/g. Injection of a higher dose of acetazolamide (20 mg/kg) showed further reduction in tumour and selected organs, but was comparable to 10 mg/kg dose.

Longitudinal imaging: uptake of ^{68}Ga-DOTA-AEBSA is correlated with tumour growth

Positive correlation between hypoxia and CA-IX expression has previously been demonstrated using PET hypoxia tracers and CA-IX immunohistochemical staining (29), but not vice versa due to the lack of suitable CA-IX tracers. Using ^{68}Ga-DOTA-AEBSA as the imaging tracer, PET studies were performed at 17, 24 and 33 days after cell-inoculation for one mouse which exhibited slower tumour growth compared to other subjects (Figure 4). Absolute uptake and overall contrast improved as the tumour grew over the three imaging sessions. Tumour size and hottest 2 × 2 voxel cluster (based on drawn ROIs) were 91.8 mm^3 and 0.21 %ID/g, 830.9 mm^3 and 0.40 %ID/g, and 1225.1 mm^3 and 0.65 %ID/g for 17, 24, and 33 days, respectively. By the second and third imaging session, distribution of radioactivity in tumour is visibly heterogeneous with several areas of focality. While additional studies are needed to determine if uptake of ^{68}Ga-DOTA-AEBSA corresponds to the degree of hypoxia, the clinical utility of tracers will be improved if they can serve as surrogate hypoxia imaging agents. As CA-IX is an endogenous marker of hypoxia, tumours that express CA-IX are not only susceptible to emergent CA-IX inhibitors, but to hypoxia-targeting therapies as well.

^{68}Ga-labeled benzenesulfonamides represent a significant advancement over reported attempts to image CA-IX using small molecule inhibitors

Historically the clinical detection of CA-IX has mainly been facilitated by CA-IX specific mAbs: M75 and cG250. Both mAbs bind to the proteoglycan-like domain of CA-IX and have been explored for use as imaging agents. ^{125}I-M75 was used for pre-clinical imaging studies (30,31), and is now commercially available as part of an enzyme-linked immunosorbent assay kit from Siemens (32). On the other hand, cG250 (RENCAREX®, WILEX AG) has been radiolabeled with an assortment of imaging isotopes including ^{124}I, ^{111}In, and ^{89}Zr (33-35). ^{124}I-cG250 advanced to Phase III clinical trials for the diagnosis of clear cell renal cell carcinoma with PET (33). Despite the success of these mAbs, there is significant interest in developing small molecule inhibitors for imaging CA-IX in vivo. The high molecular weight of mAbs, combined with tumour interstitial pressure and aberrant vasculature, could limit tissue penetrance and ability to bind CA-IX.

The development of CA-IX inhibitors as PET imaging agents have been met with limited success. Those that have been evaluated in the pre-clinical setting have shown low tumour uptake, lack of isoform selectivity, and/or instability in vivo (36-39). Recently, we reported the synthesis and biological evaluations of four ^{18}F-labeled sulfonamide derivatives for CA-IX imaging (19). For each tracer, HT-29 tumour xenografts were readily visualized with modest contrast (tumour-to-muscle ratios of 3.18-9.55). In vivo selectivity for CA-IX was achieved through the use of a multivalent design; however, absolute uptake in tumour remained low (0.30-0.64 %ID/g at 1 h p.i.). Furthermore, high sequestration of activity in liver and GI tract precludes their use for imaging lesions in these organs. By comparison, all three tracers presented in this paper had higher absolute uptake with comparable contrasts. ^{68}Ga-DOTA-AEBSA and to a lesser extent ^{68}Ga-DOTA-$(AEBSA)_2$ showed favourable pharmacokinetic profiles that will enable detection of lesions within the abdominal thorax. To the best of our knowledge, this paper describes the first series of sulfonamide-based tracers radiolabeled with ^{68}Ga that is

successful for CA-IX imaging. Given the prognostic and therapeutic significance of CA-IX, we believe that polyaminocarboxylate chelator-conjugated sulfonamides will warrant further investigation for potential translation to the clinic upon further optimization.

CONCLUSION

We have demonstrated that ^{68}Ga-labeled benzenesulfonamide inhibitors can be used for non-invasive imaging of CA-IX. Easily produced, with favourable pharmacokinetics and rapid tumour targeting, these tracers represent attractive alternatives to conventional mAb-based imaging systems. Clinically, these nanomolar affinity compounds will enable physicians to determine if patients' tumours express sufficiently high levels of CA-IX to make them candidates for personalized treatments targeting this protein. As CA-IX is considered an endogenous marker for hypoxia in certain cancer subtypes, correlative imaging studies with established hypoxia PET tracers like ^{18}F-MISO or ^{18}F-EF5 would be yield valuable information.

ACKNOWLEDGEMENTS

This work was financially supported by the Canadian Cancer Society, the Canadian Institutes of Health Research, and the Leading Edge Endowment Fund, including a Rix Family scholarship. The authors would like to acknowledge Navjit Hundal-Jabal and Nadine Colpo for their assistance with imaging studies.

REFERENCES

1. Harris AL. Hypoxia--a key regulatory factor in tumour growth. Nature reviews Cancer 2002;2(1):38-47.
2. McDonald PC, Dedhar S. Carbonic anhydrase IX (CAIX) as a mediator of hypoxia-induced stress response in cancer cells. Sub-cellular biochemistry 2014;75:255-69.
3. Wilson WR, Hay MP. Targeting hypoxia in cancer therapy. Nature reviews Cancer 2011;11(6):393-410.
4. Swietach P, Hulikova A, Vaughan-Jones RD, Harris AL. New insights into the physiological role of carbonic anhydrase IX in tumour pH regulation. Oncogene 2010;29(50):6509-21.
5. Robertson N, Potter C, Harris AL. Role of carbonic anhydrase IX in human tumor cell growth, survival, and invasion. Cancer research 2004;64(17):6160-5.
6. Supuran CT. Carbonic anhydrases: novel therapeutic applications for inhibitors and activators. Nature reviews Drug discovery 2008;7(2):168-81.
7. Monti SM, Supuran CT, De Simone G. Anticancer carbonic anhydrase inhibitors: a patent review (2008 - 2013). Expert opinion on therapeutic patents 2013;23(6):737-49.
8. Weissleder R, Mahmood U. Molecular imaging. Radiology 2001;219(2):316-33.
9. Cherry SA, Sorenson JA, Phelps ME. Physics in nuclear medicine. 4th ed. Philadelphia: Elsevier/Saunders; 2012.
10. Gambhir SS. Molecular imaging of cancer with positron emission tomography. Nature reviews Cancer 2002;2(9):683-93.
11. Kelkar SS, Reineke TM. Theranostics: combining imaging and therapy. Bioconjugate chemistry 2011;22(10):1879-903.
12. Pacchiano F, Carta F, McDonald PC, Lou Y, Vullo D, Scozzafava A, et al. Ureido-substituted benzenesulfonamides potently inhibit carbonic anhydrase IX and show antimetastatic activity in a model of breast cancer metastasis. Journal of medicinal chemistry 2011;54(6):1896-902.
13. Lin KS, Pan J, Amouroux G, Turashvili G, Mesak F, Hundal-Jabal N, et al. In vivo radioimaging of bradykinin receptor b1, a widely overexpressed molecule in human cancer. Cancer research 2015;75(2):387-93.
14. Neri D, Supuran CT. Interfering with pH regulation in tumours as a therapeutic strategy. Nature reviews Drug discovery 2011;10(10):767-77.
15. Cecchi A, Hulikova A, Pastorek J, Pastorekova S, Scozzafava A, Winum JY, et al. Carbonic anhydrase inhibitors. Design of fluorescent sulfonamides as probes of tumor-associated carbonic anhydrase IX that inhibit isozyme IX-mediated acidification of hypoxic tumors. Journal of medicinal chemistry 2005;48(15):4834-41.
16. Ahlskog JK, Dumelin CE, Trussel S, Marlind J, Neri D. In vivo targeting of tumor-associated carbonic anhydrases using acetazolamide derivatives. Bioorganic & medicinal chemistry letters 2009;19(16):4851-6.
17. Dubois L, Douma K, Supuran CT, Chiu RK, van Zandvoort MA, Pastorekova S, et al. Imaging the hypoxia surrogate marker CA IX requires expression and catalytic activity for binding fluorescent sulfonamide inhibitors. Radiotherapy and

oncology : journal of the European Society for Therapeutic Radiology and Oncology 2007;83(3):367-73.
18. Wilkinson BL, Bornaghi LF, Houston TA, Innocenti A, Supuran CT, Poulsen SA. A novel class of carbonic anhydrase inhibitors: glycoconjugate benzene sulfonamides prepared by "click-tailing". Journal of medicinal chemistry 2006;49(22):6539-48.
19. Lau J, Liu Z, Lin KS, Pan J, Zhang Z, Vullo D, et al. Trimeric radiofluorinated sulfonamide derivatives to achieve in vivo selectivity for carbonic anhydrase IX-targeted PET imaging. Journal of nuclear medicine : official publication, Society of Nuclear Medicine 2015.
20. Casey JR, Morgan PE, Vullo D, Scozzafava A, Mastrolorenzo A, Supuran CT. Carbonic anhydrase inhibitors. Design of selective, membrane-impermeant inhibitors targeting the human tumor-associated isozyme IX. Journal of medicinal chemistry 2004;47(9):2337-47.
21. Scozzafava A, Briganti F, Ilies MA, Supuran CT. Carbonic anhydrase inhibitors: synthesis of membrane-impermeant low molecular weight sulfonamides possessing in vivo selectivity for the membrane-bound versus cytosolic isozymes. Journal of medicinal chemistry 2000;43(2):292-300.
22. Rami M, Cecchi A, Montero JL, Innocenti A, Vullo D, Scozzafava A, et al. Carbonic anhydrase inhibitors: design of membrane-impermeant copper(II) complexes of DTPA-, DOTA-, and TETA-tailed sulfonamides targeting the tumor-associated transmembrane isoform IX. ChemMedChem 2008;3(11):1780-8.
23. Rami M, Winum JY, Innocenti A, Montero JL, Scozzafava A, Supuran CT. Carbonic anhydrase inhibitors: copper(II) complexes of polyamino-polycarboxylamido aromatic/heterocyclic sulfonamides are very potent inhibitors of the tumor-associated isoforms IX and XII. Bioorganic & medicinal chemistry letters 2008;18(2):836-41.
24. Dilworth JR, Pascu SI, Waghorn PA, Vullo D, Bayly SR, Christlieb M, et al. Synthesis of sulfonamide conjugates of Cu(II), Ga(III), In(III), Re(V) and Zn(II) complexes: carbonic anhydrase inhibition studies and cellular imaging investigations. Dalton transactions 2015;44(11):4859-73.
25. Anderson CJ, Ferdani R. Copper-64 radiopharmaceuticals for PET imaging of cancer: advances in preclinical and clinical research. Cancer biotherapy & radiopharmaceuticals 2009;24(4):379-93.
26. Fani M, Andre JP, Maecke HR. 68Ga-PET: a powerful generator-based alternative to cyclotron-based PET radiopharmaceuticals. Contrast media & molecular imaging 2008;3(2):67-77.
27. Berry DJ, Ma Y, Ballinger JR, Tavare R, Koers A, Sunassee K, et al. Efficient bifunctional gallium-68 chelators for positron emission tomography: tris(hydroxypyridinone) ligands. Chemical communications 2011;47(25):7068-70.
28. Maecke HR, Hofmann M, Haberkorn U. (68)Ga-labeled peptides in tumor imaging. Journal of nuclear medicine : official publication, Society of Nuclear Medicine 2005;46 Suppl 1:172S-8S.
29. Carlin S, Zhang H, Reese M, Ramos NN, Chen Q, Ricketts SA. A comparison of the imaging characteristics and microregional distribution of 4 hypoxia PET

tracers. Journal of nuclear medicine : official publication, Society of Nuclear Medicine 2014;55(3):515-21.
30. Chrastina A, Pastorekova S, Pastorek J. Immunotargeting of human cervical carcinoma xenograft expressing CA IX tumor-associated antigen by 125I-labeled M75 monoclonal antibody. Neoplasma 2003;50(1):13-21.
31. Chrastina A, Zavada J, Parkkila S, Kaluz S, Kaluzova M, Rajcani J, et al. Biodistribution and pharmacokinetics of 125I-labeled monoclonal antibody M75 specific for carbonic anhydrase IX, an intrinsic marker of hypoxia, in nude mice xenografted with human colorectal carcinoma. International journal of cancer Journal international du cancer 2003;105(6):873-81.
32. Wind TC, Messenger MP, Thompson D, Selby PJ, Banks RE. Measuring carbonic anhydrase IX as a hypoxia biomarker: differences in concentrations in serum and plasma using a commercial enzyme-linked immunosorbent assay due to influences of metal ions. Annals of clinical biochemistry 2011;48(Pt 2):112-20.
33. Divgi CR, Uzzo RG, Gatsonis C, Bartz R, Treutner S, Yu JQ, et al. Positron emission tomography/computed tomography identification of clear cell renal cell carcinoma: results from the REDECT trial. Journal of clinical oncology : official journal of the American Society of Clinical Oncology 2013;31(2):187-94.
34. Stillebroer AB, Franssen GM, Mulders PF, Oyen WJ, van Dongen GA, Laverman P, et al. ImmunoPET imaging of renal cell carcinoma with (124)I- and (89)Zr-labeled anti-CAIX monoclonal antibody cG250 in mice. Cancer biotherapy & radiopharmaceuticals 2013;28(7):510-5.
35. Stillebroer AB, Zegers CM, Boerman OC, Oosterwijk E, Mulders PF, O'Donoghue JA, et al. Dosimetric analysis of 177Lu-cG250 radioimmunotherapy in renal cell carcinoma patients: correlation with myelotoxicity and pretherapeutic absorbed dose predictions based on 111In-cG250 imaging. Journal of nuclear medicine : official publication, Society of Nuclear Medicine 2012;53(1):82-9.
36. Pan J, Lau J, Mesak F, Hundal N, Pourghiasian M, Liu Z, et al. Synthesis and evaluation of 18F-labeled carbonic anhydrase IX inhibitors for imaging with positron emission tomography. Journal of enzyme inhibition and medicinal chemistry 2014;29(2):249-55.
37. Lau J, Pan J, Zhang Z, Hundal-Jabal N, Liu Z, Benard F, et al. Synthesis and evaluation of (18)F-labeled tertiary benzenesulfonamides for imaging carbonic anhydrase IX expression in tumours with positron emission tomography. Bioorganic & medicinal chemistry letters 2014;24(14):3064-8.
38. Sneddon D, Poulsen SA. Agents described in the Molecular Imaging and Contrast Agent Database for imaging carbonic anhydrase IX expression. Journal of enzyme inhibition and medicinal chemistry 2014;29(5):753-63.
39. Peeters SG, Dubois L, Lieuwes NG, Laan D, Mooijer M, Schuit RC, et al. [F]VM4-037 MicroPET Imaging and Biodistribution of Two In Vivo CAIX-Expressing Tumor Models. Molecular imaging and biology : MIB : the official publication of the Academy of Molecular Imaging 2015.

Table 1. Binding affinity (K_i) of sulfonamide inhibitors to CA-I, CA-II, CA-IX and CA-XII were determined via a stopped-flow CO_2 hydration assay.

	Ki affinity (nM)*			
	CA-I	**CA-II**	**CA-IX**	**CA-XII**
Ga-DOTA-AEBSA	38.0	136.8	10.8	30.7
Ga-DOTA-(AEBSA)$_2$	37.6	41.2	25.4	7.4
Ga-NOTGA-(AEBSA)$_3$	34.4	7.2	7.7	6.5
Acetazolamide	250	12.0	25.0	6.0

*Errors in the range of 5-10% of the reported value from three different assays.

Table 2. Molecular weight, radiolabeling, LogD7.4, and plasma stability of ^{68}Ga CA-IX inhibitors.

	Molecular Weight (dalton)	**% Isolated Radiochemical Yield[a]**	**% Radiochemical Purity**	**Specific Activity (GBq/μmol)**	**$LogD_{7.4}$ (Octanol/PBS)**	**Stability in Plasma after 2h (% intact)**
^{68}Ga-DOTA-AEBSA	653.36	91 ± 3	97.5 ± 1.9	536.5 ± 187.1	-4.37 ± 0.08	> 91
^{68}Ga-DOTA-$(AEBSA)_2$	835.6	84 ± 4	97.8 ± 1.8	269.5 ± 176.9	-3.52 ± 0.01	> 96
^{68}Ga-NOTGA-$(AEBSA)_3$	1132.93	64 ± 8	99.3 ± 0.3	50.9 ± 8.4	-2.39 ± 0.01	> 92

Perimeters are presented as mean values ± standard deviation (n ≥3), except for plasma stability (n =1).

[a]Decay-corrected.

Table 3. Biodistribution and tumour to non-target ratios for ^{68}Ga CA-IX inhibitors

Organ	**^{68}Ga-DOTA-AEBSA**			**^{68}Ga-DOTA-(AEBSA)$_2$**	**^{68}Ga-NOTGA-(AEBSA)$_3$**
	Unblocked (n=5)	**10 mg/kg AZA**[a] (n=5)	**20 mg/kg AZA**[a] (n=4)	**Unblocked** (n=5)	**Unblocked** (n=5)
Blood	0.63 ± 0.15	0.33 ± 0.13[b]	0.25 ± 0.08[b]	1.53 ± 0.25	0.92 ± 0.35
Fat	0.09 ± 0.04	0.08 ± 0.07	0.04 ± 0.01[b]	0.24 ± 0.13	0.21 ± 0.14
Testes	0.16 ± 0.05	0.10 ± 0.05	0.06 ± 0.02[b]	0.41 ± 0.06	0.37 ± 0.09
Stomach	0.17 ± 0.07	0.14 ± 0.12	0.24 ± 0.33	0.77 ± 0.34	2.77 ± 1.74
Spleen	0.25 ± 0.05	0.16 ± 0.07[b]	0.07 ± 0.02[b]	1.77 ± 1.44	1.08 ± 0.54
Liver	0.83 ± 0.29	0.48 ± 0.08[b]	0.32 ± 0.10[b]	3.78 ± 1.06	8.01 ± 3.58
Pancreas	0.15 ± 0.04	0.08 ± 0.02[b]	0.05 ± 0.01[b]	0.49 ± 0.21	0.46 ± 0.11
Adrenals	0.40 ± 0.06	0.32 ± 0.25	0.08 ± 0.03[b]	1.23 ± 0.51	1.16 ± 0.61
Kidney	4.37 ± 1.04	1.92 ± 0.46[b]	1.28 ± 0.32[b]	14.84 ± 7.21	14.40 ± 1.65
Lungs	0.56 ± 0.13	0.32 ± 0.13[b]	0.16 ± 0.05[b]	1.86 ± 0.37	2.27 ± 0.44
Heart	0.20 ± 0.07	0.12 ± 0.04	0.12 ± 0.04	0.67 ± 0.15	0.70 ± 0.18
Muscle	0.16 ± 0.03	0.08 ± 0.03[b]	0.09 ± 0.11	0.49 ± 0.10	0.56 ± 0.15
Bone	0.20 ± 0.05	0.22 ± 0.16	0.04 ± 0.01[b]	0.60 ± 0.24	0.40 ± 0.27
Brain	0.05 ± 0.01	0.04 ± 0.03	0.01 ± 0.00[b]	0.11 ± 0.06	0.07 ± 0.03
Tumour	**0.81 ± 0.15**	**0.41 ± 0.10[b]**	**0.35 ± 0.17[b]**	**1.93 ± 0.26**	**2.30 ± 0.53**
Tumour/liver	1.03 ± 0.21	0.85 ± 0.16	1.04 ± 0.22	0.48 ± 0.15	0.30 ± 0.05
Tumour/blood	1.29 ± 0.11	1.31 ± 0.26	1.37 ± 0.24	1.28 ± 0.18	2.67 ± 0.72
Tumour/muscle	5.02 ± 0.22	5.63 ± 1.52	6.26 ± 2.74	4.07 ± 0.87	4.18 ± 0.84

Biodistribution and ratios are at 1 h post-injection. Values are presented as mean ± standard deviation.
[a]Blocked by pre-injection of acetazolamide 1 h before administering radiotracer.
[b]Pre-injection significantly reduced uptake of the same organ for the tracer ($p<0.05$)

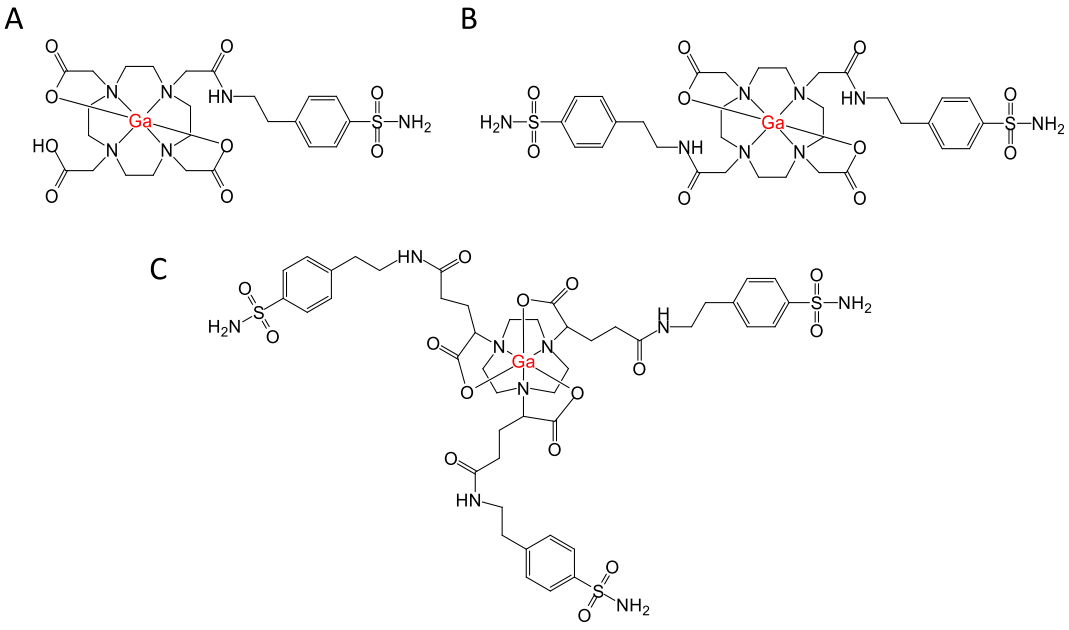

Figure 1. Inhibition of CA-IX with benzenesulfonamide derivatives. Chemical structures of CA-IX inhibitors used in this study: **(A)** DOTA-AEBSA, **(B)** DOTA-$(AEBSA)_2$ and **(C)** NOTGA-$(AEBSA)_3$.

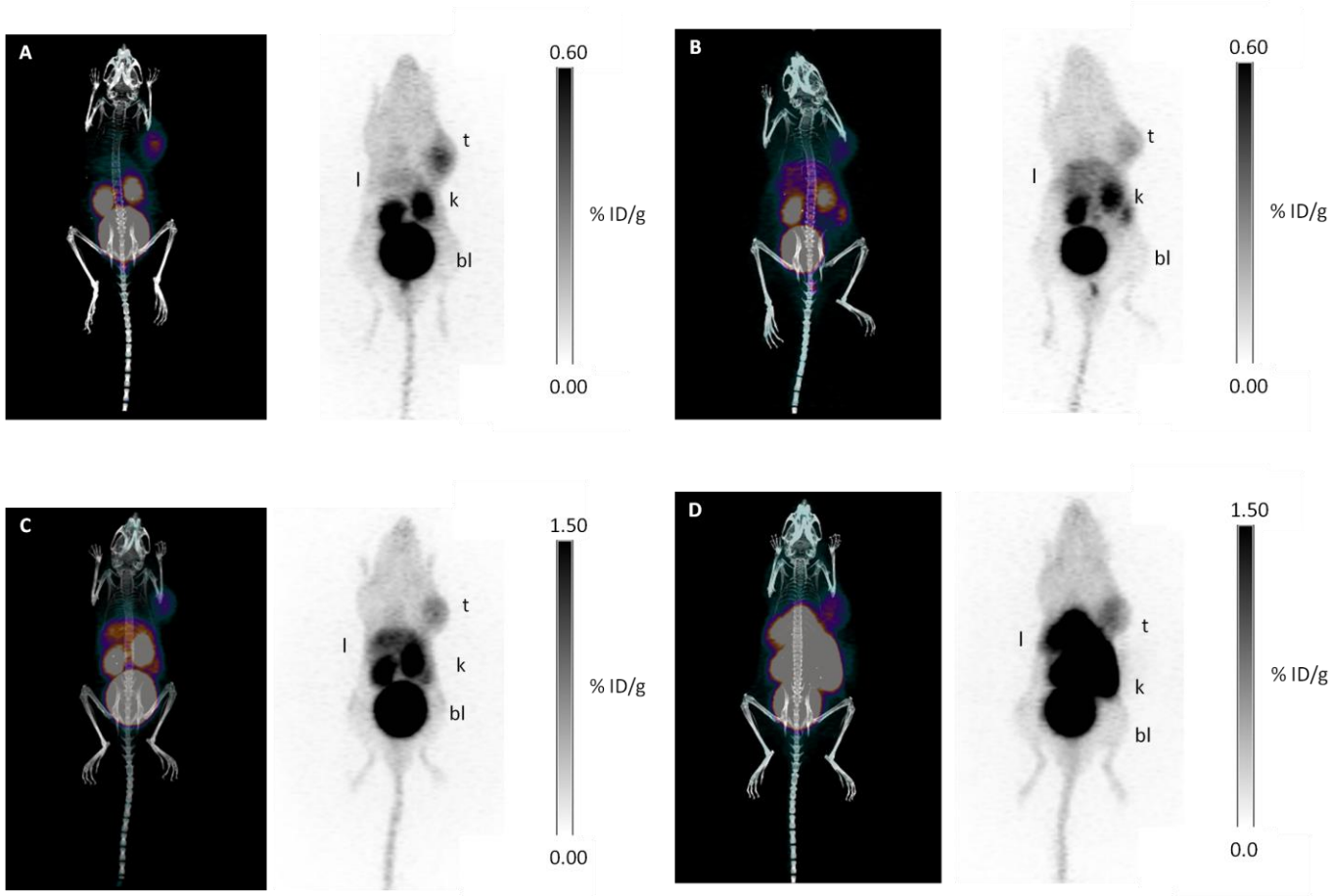

Figure 3. Maximal intensity projections of PET/CT and PET with ^{68}Ga tracers at 1 h post-injection. (A) ^{68}Ga-DOTA-AEBSA; (B): ^{68}Ga-DOTA-AEBSA pre-blocked with 10 mg/kg of acetazolamide; **(C)**: ^{68}Ga-DOTA-$(AEBSA)_2$; and **(D)**: ^{68}Ga-NOTGA-$(AEBSA)_3$. Tumour uptake was observed for all three compounds with ^{68}Ga-DOTA-AEBSA displaying highest contrast. t = tumour; l = liver; k = kidney; bl = bladder

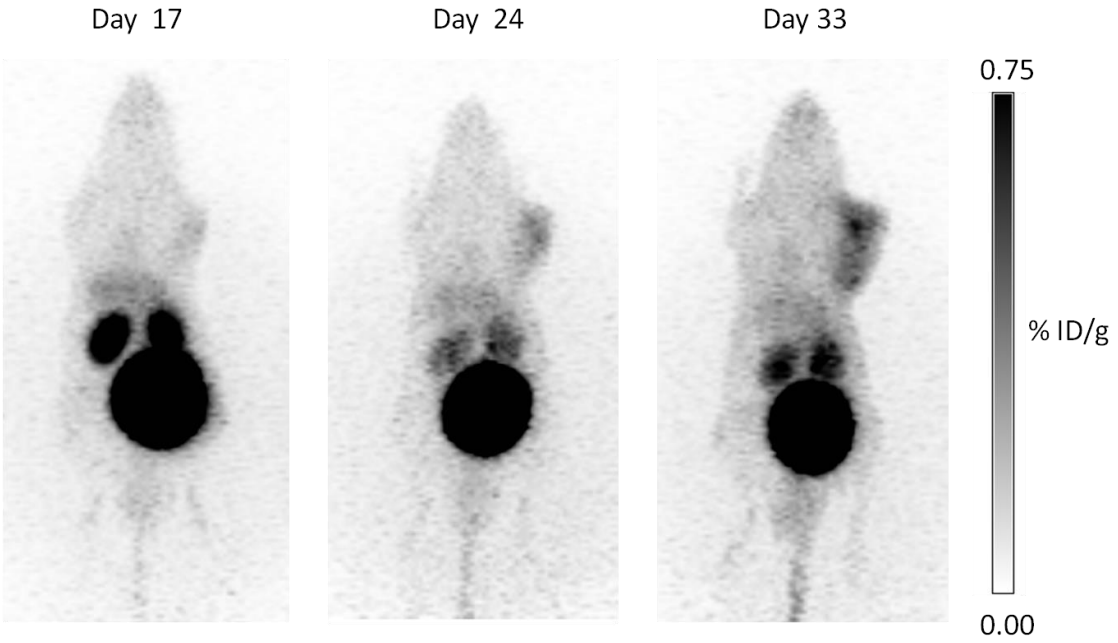

Figure 4. Longitudinal study: uptake of ^{68}Ga-DOTA-AEBSA in HT-29 tumour xenograft increases as tumour grows. Tumour bearing mice was imaged 17, 24 and 33 days post-cell inoculation with ^{68}Ga-DOTA-AEBSA.